G. R. MacCartney, Jr., M. K. Samimi, T. S. Rappaport, "Omnidirectional Path Loss Models in New York City at 28 GHz and 73 GHz," in *2014 IEEE 25th International Symposium on Personal Indoor and Mobile Radio Communications (PIMRC),* Sept 2 - 5, 2014.

# Omnidirectional Path Loss Models in New York City at 28 GHz and 73 GHz

George R. MacCartney Jr., Mathew K. Samimi, and Theodore S. Rappaport
NYU WIRELESS
NYU Polytechnic School of Engineering
Brooklyn, NY 11201
{gmac, mks, tsr}@nyu.edu

***Abstract*—This paper presents newly generated omnidirectional close-in free space reference distance and floating intercept path loss models obtained from 28 GHz and 73 GHz RF ultra-wideband propagation measurements collected in Downtown Manhattan using a 400 Mega-chip-per-second sliding correlator channel sounder. Simplified path loss models with respect to a 1 m close-in free space reference distance are provided here for the omnidirectional propagation models, and are suitable for system-wide simulations similar to 3GPP and WINNER II. Measured path loss exponents at millimeter-wave and current UHF/Microwave cellular frequencies are very similar. The significant difference in large-scale path loss between UHF and millimeter-wave channels is the extra free space attenuation due to the increase in carrier frequency.**

***Index Terms*—mmWave; 5G; omnidirectional; path loss; propagation.**

## I. Introduction

Radio-system engineers require omnidirectional path loss models to estimate the total received power at a given transmitter-receiver (T-R) separation distance, as perceived from two omnidirectional isotropic transmit and receive antennas with 0 dBi gain, that allow them to superimpose arbitrary antenna patterns for studying various channels with different types of antennas. To date, extensive omnidirectional path loss models have been developed based on propagation measurements to model path loss as a function of many parameters including distance, frequency, antenna beamwidth, and transmitter and receiver heights [1].

The 3GPP and WINNER II statistical spatial channel models (SSCMs) provide such omnidirectional path loss models by fitting a minimum mean square error (MMSE) best fit line to the measured path losses (with distances in log-scale), yielding a mathematically-based omnidirectional path loss model, applicable over the range of measured distances, a so called *floating-intercept* model. This model is in direct contrast with the other widely used *close-in free space reference distance* path loss model used in characterizing radio-propagation environments, arising from electromagnetic theory, and uses a close-in free space reference distance $d_0$ over which free space propagation is assumed. The close-in free space reference distance model is obtained using a constraint anchor point at the close-in reference distance $d_0$ (assuming free space propagation up to $d_0$) when fitting the MMSE best fit line, where the slope of the best fit line and standard deviation beyond $d_0$ are commonly known as the *path loss exponent* (PLE) and *shadowing factor*, respectively. The floating intercept model is derived similarly; however, without the anchor point constraint. The parameters used in the close-in free space reference distance model provide physical insight into channel propagation characteristics as compared to free space propagation, contrary to the floating-intercept model, which simply provides a best minimum error fit to collected path losses.

Many 3G and 4G MIMO radio systems are designed using the geometry-based stochastic 3GPP and WINNER II SSCMs that provide channel coefficients based on real-world propagation measurements in many types of environments conducted between 1 GHz and 6 GHz and for RF signal bandwidths spanning 5 MHz to 100 MHz [2] [3]. These UHF/Microwave models are not accurate for channels at millimeter-wave (mmWave) frequencies with much larger bandwidths (time delay resolution smaller than 20 ns) and narrower angular resolution (narrowbeam pointing capabilities) [4].

Knowledge of omnidirectional propagation channel characteristics for mmWave mobile and backhaul broadband communication applications in dense urban environments is lacking. Previous published results in [5]–[7] showed 28 GHz and 73 GHz *directional* path loss models used in estimating path loss at unique pointing angles, as opposed to omnidirectional models which allow one to estimate the total received omnidirectional power. Samsung's DMC R&D research team recently conducted measurements at 28 GHz using rotatable horn antennas with 24.5 dBi gain in NLOS environments, revealing an omnidirectional path loss exponent of 4.82 and shadowing factor of 5.64 dB with respect to a 5 m close-in free space reference distance [8].

Extensive 28 GHz and 73 GHz wideband propagation measurements were carried out in New York City to investigate and assess the viability of next generation mmWave mobile and backhaul broadband communications in dense urban environments [5]–[7]. These measurements provide the necessary basis for developing mmWave omnidirectional and spatial channel models which must account for the order of magnitude increase in both carrier frequency and RF bandwidths involved to accommodate the widespread demand for faster data rates [9]. We present here omnidirectional path loss models using the floating-intercept and close-in free space reference distance

path loss models at 28 GHz and 73 GHz obtained from ultra-wideband 800 MHz RF null-to-null bandwidth measurements in Manhattan, needed for standard bodies in designing next generation radio-systems for arbitrary antenna patterns.

## II. Measurement Hardware and Procedures

The 28 GHz and 73 GHz measurements were collected in Manhattan with a 400 Mcps broadband sliding correlator channel sounder and highly directional 24.5 dBi and 27 dBi (10.9° and 7° half-power beamwidths, respectively) gain horn antennas, which were steered in incremental steps of one antenna beamwidth in the azimuth plane for various elevation planes to investigate angle of departure (AOD) and angle of arrival (AOA) statistics. Fig. 1 shows the RF front end up-converter equipment mounted on top of an electrically-steered rotatable gimbal used in Downtown Manhattan during the 73 GHz measurement campaign. Thousands of power delay profiles (PDPs) were collected at many azimuth and elevation angle combinations so as to develop spatial and temporal mmWave channel models. Table I shows the specifications for the two sets of channel sounders used at 28 GHz and 73 GHz, and additional details pertaining to the measurement campaigns can be found in [5] [7] [10].

## III. Theoretical Path Loss Models

Omnidirectional path loss at an arbitrary distance $d$ may be estimated using the close-in free space reference distance model, as shown in Eq. 1:

$$\mathrm{PL}(d)[\mathrm{dB}] = \mathrm{PL}(d_0) + 10\,\overline{n}\log_{10}\left(\frac{d}{d_0}\right) + X_\sigma \quad (d \geq d_0) \quad (1)$$

where,

$$\mathrm{PL}[\mathrm{dB}](d_0) = 20\log_{10}\left(\frac{4\pi d_0}{\lambda}\right) \quad (2)$$

$$\lambda = \frac{c}{f_c} \quad (3)$$

where $d_0$ (m) is the free space reference distance, $\lambda$ (m) is the carrier wavelength, $c = 3 \times 10^8$ m/s, $f_c$ (Hz) is the RF carrier frequency, $\overline{n}$ is the path loss exponent, and $X_\sigma$ is the typical log-normal random variable with 0 dB mean and standard deviation $\sigma$ that models large scale fading [11]. Note that $\mathrm{PL}(d_0)$ in Eq. 1 models the frequency dependence through $\lambda$. In this work, we specify $d_0 = 1$ m for simplicity.

The floating-intercept model is currently used in standards work such as 3GPP and WINNER II, and is shown below:

$$\mathrm{PL}[\mathrm{dB}] = \alpha + 10 \cdot \beta \log_{10}(d) + X_\sigma \quad (4)$$

where $X_\sigma$ is the log-normal random variable with 0 dB mean and standard deviation $\sigma$ [12]. The WINNER II path loss model is a floating-intercept model, and is shown below [13]:

$$\mathrm{PL} = A\log_{10}(d[\mathrm{m}]) + B + C\log_{10}\left(\frac{f_c[\mathrm{GHz}]}{5.0}\right) + X \quad (5)$$

where $A$ is a fitting parameter that includes the path loss exponent, $B$ is the incercept, $C$ is a path loss frequency-dependent parameter, and $X$ is an environment-specific term [13]. This model is frequency-dependent between 2-6 GHz.

TABLE I: Channel sounder hardware specifications for 28 and 73 GHz measurements in New York City.

| | 28 GHz Campaign | 73 GHz Campaign |
|---|---|---|
| Carrier Frequency | 28 GHz | 73.5 GHz |
| Probing Sequence | $11^{th}$ order PN Code (L = 2047) | |
| TX Chip Rate | 400 Mcps | |
| RX Chip Rate | 399.95 Mcps | |
| Slide Factor | $\gamma$ = 8000 | |
| TX Ant. Gain | 24.5 dBi | 27 dBi |
| TX Ant. AZ HPBW | 10.9° | 7° |
| TX Ant. EL HPBW | 8.6° | 7° |
| RX Ant. Gain | 24.5 dBi | 27 dBi |
| RX Ant. AZ HPBW | 10.9° | 7° |
| RX Ant. EL HPBW | 8.6° | 7° |
| Ant. Polarization | V-to-V | |
| Max TX Power | 30 dBm | 14.6 dBm |
| Max Measurable Path Loss | 178 dB | 181 dB |

Fig. 1: 73 GHz channel sounder RF front-end upconverter with a 20 dBi gain (15° beamwidth) directional horn antenna (used for indoor measurements in a typical office environment), mounted to a degree-precision LabVIEW-controlled FLIR gimbal. The gimbal is mounted to a pneumatic mast that lifts the RF front-end to backhaul heights up to 4 m.

## IV. Synthesizing Omnidirectional Models

The 28 GHz propagation measurements at each RX location consisted of 10 antenna pointing combinations, for nine RX azimuthal sweeps where the RX antenna was rotated in 10° azimuthal increments for three pre-determined elevation planes of 0° (parallel to the horizon) and ±20°, for fixed TX azimuth and -10° elevation downtilt. The 10th pointing angle measurement investigated AODs by sweeping the TX antenna in the azimuth plane for fixed -10° elevation, and for a fixed RX antenna pointing angle [5]. The 28 GHz omnidirectional path losses were obtained by summing all received powers (e.g. the area under the curve of each PDP for each pointing angle) for each unique azimuth and elevation pointing angle combination at each TX-RX location combination, and removing TX and RX antenna gains for each individual PDP recording. For the 73 GHz measurements, the use of a narrower antenna beamwidth (7°) resulted in a maximum of 540 PDPs for each TX-RX combination. Measurement details pertaining to the 73 GHz measurement campaign [7] are very similar to the 28 GHz measurement details presented above.

The 28 GHz nine AOA measurements were performed for three adjacent TX azimuth angles, separated by 5° with an elevation downtilt of -10°. Since the 24.5 dBi antennas used had 10° half-power beamwidths, the powers summed at the RX's contained overlapping energy from the three separate TX azimuth angles, and the path losses computed are therefore optimistic if compared to three different TX azimuth angles that had no overlap. However, the optimistic use of closely spaced TX beams is expected to make up for different wider spacing in both the azimuth and elevation planes that were never measured, but would have likely completed a link at the RX, that would produce energy and would be added to the received signal for a true omnidirectional TX antenna. Since each measurement configuration consisted of sweeping the antenna in 10° step increments, a maximum of 36 possible individual PDPs could be recorded for each sweep, with up to 360 measured channel impulse responses when considering all 10 measurement configurations for a given TX-RX location combination. Note that when summing all received powers from every unique pointing angle measured, double counting arising from the TX sweep and one of the nine RX sweeps was carefully removed.

The initial results for our 73 GHz 3GPP-like omnidirectional path loss model reported in [14] summed received powers for access and backhaul RX antenna heights into one receiver (thereby approximately doubling the power as seen by a receiver at a height of 2 m or 4.06 m). In this paper, we provide the omnidirectional path loss models for separate access and backhaul heights, as well as the "hybrid" path loss model for considering both access and backhaul heights, in both LOS and NLOS environments.

## V. Path Loss Models

Fig. 2 and Fig. 3 show the 28 GHz and 73 GHz path loss scatter plots and close-in free space reference distance omnidirectional path loss models in LOS and NLOS environments, and the floating intercept model for the NLOS environment. Table II defines the LOS and NLOS propagation environment types. The close-in free space reference distance path loss model at 1900 MHz from [15] with a RX height of 1.7 m and a TX height of 8.5 m in an obstructed environment in San Francisco with path loss exponent $\overline{n}$ = 2.6 and shadowing factor $\sigma_{\mathrm{SF}} = 7.8$ dB, is also included. The 28 GHz and 73 GHz LOS path loss exponents with respect to a 1 m free space reference distance were found to be 2.1 and 2.0, respectively. The 28 GHz LOS measurements were not obtained with TX and RX antennas aligned on boresight as the angle configurations were pre-determined before the measurement campaign, explaining the larger than free space ($n = 2$) path loss exponent, while at 73 GHz the antennas were aligned on boresight in LOS environments. Experience taught us later for the 73 GHz measurements that it was better to always point the TX and RX antennas on boresight. The 28 GHz and 73 GHz (hybrid) NLOS path loss exponents were determined to be 3.4. Fig. 2 and Fig. 3 show the close-in reference and floating intercept best fit lines that estimate NLOS path loss.

Table III summarizes the channel model parameters for the

TABLE II: Path loss terminology description for omnidirectional models.

| Setting | Description |
|---|---|
| LOS | Path loss when the TX and RX sites have a clear line-of-sight between each other. The antennas may not be boresight-to-boresight, but there are no obstructions between them. |
| NLOS | Path loss when the TX and RX sites are separated by obstructions and there is no clear direct path between the antennas. |

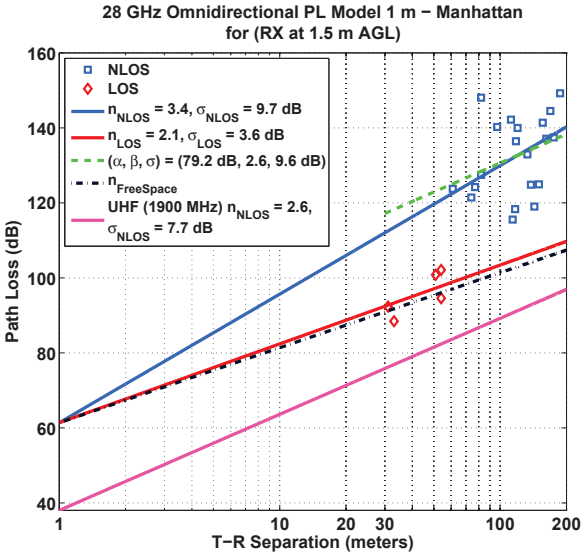


Fig. 2: 28 GHz omnidirectional close-in free space reference distance ($d_0 = 1$ m) and floating intercept (NLOS) path loss models with the RX antenna at a height of 1.5 m above ground level (AGL) in the dense urban environment of New York City.

TABLE III: Close-in free space space reference distance ($d_0 = 1$ m) and floating intercept path loss models for base station-to-mobile (access) and base station-to-base station (backhaul) scenarios. PLE is the path loss exponent, $\alpha$ is the floating intercept in dB, $\beta$ is the slope of the MMSE best fit line, and $\sigma$ is the standard deviation in dB.

| Omnidirectional Path Loss Models ($d_0 = 1$ m) | | | | | | | | | | |
|---|---|---|---|---|---|---|---|---|---|---|
| | | TX Height (m) | RX Height (m) | LOS | | NLOS | | NLOS (Floating) 30 m < d < 200 m | | |
| | | | | PLE | $\sigma$ [dB] | PLE | $\sigma$ [dB] | $\alpha$ [dB] | $\beta$ | $\sigma$ [dB] |
| 28 GHz | Access | 7; 17 | 1.5 | 2.1 | 3.6 | 3.4 | 9.7 | 79.2 | 2.6 | 9.6 |
| 73 GHz | Access | 7; 17 | 2 | 2.0 | 5.2 | 3.3 | 7.6 | 81.9 | 2.7 | 7.5 |
| | Backhaul | | 4.06 | 2.0 | 4.2 | 3.5 | 7.9 | 84.0 | 2.8 | 7.8 |
| | Hybrid | | 2; 4.06 | 2.0 | 4.8 | 3.4 | 7.9 | 80.6 | 2.9 | 7.8 |

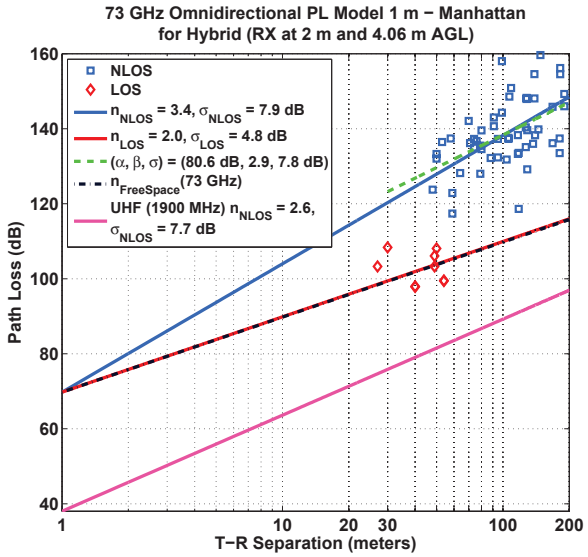


Fig. 3: 73 GHz omnidirectional close-in free space reference distance ($d_0 = 1$ m) and floating intercept (NLOS) path loss models for the hybrid scenario with the RX antenna at heights of 2 m and 4.06 m above ground level (AGL) in the dense urban environment of New York City.

close-in free space reference distance and floating intercept models for both the 28 GHz and 73 GHz bands for each specific measurement scenario. The 73 GHz measurements showed that path loss values are relatively similar for both backhaul (4.06 m) and access heights (2 m), highlighting a weak dependence upon the RX height. The NLOS path loss exponents are both $\overline{n} = 3.4$ for 28 GHz and 73 GHz measurements. At 28 GHz there was one LOS data point at a T-R separation distance of 100 m that had larger path loss than free space, but this was removed because the TX and RX antennas were not on boresight, as previously described for 28 GHz LOS measurements. Thus, the LOS omnidirectional path loss exponents are close to ($\overline{n} = 2.1$ at 28 GHz) or identical to ($\overline{n} = 2.0$ for 73 GHz access) free space propagation. Note that these LOS models are generated from a small set of data points, and must be enhanced with more LOS measurements.

The parameters shown in Table III can be used to generate 28 GHz and 73 GHz LOS and NLOS omnidirectional close-in free space reference distance path loss models required for system-level simulations and design, similar to 3GPP and WINNER II. Setting $d_0$ = 1 m, the simplified close-in free space reference equations are shown below.

$$\mathrm{PL}_{28\mathrm{GHz}}(\mathrm{LOS})[\mathrm{dB}](d) = 61.4 + 21\log_{10}(d) + X_\sigma(\sigma = 3.6\ \mathrm{dB}) \quad (6)$$

$$\mathrm{PL}_{28\mathrm{GHz}}(\mathrm{NLOS})[\mathrm{dB}](d) = 61.4 + 34\log_{10}(d) + X_\sigma(\sigma = 9.7\ \mathrm{dB}) \quad (7)$$

$$\mathrm{PL}_{73\mathrm{GHz\text{-}Hybrid}}(\mathrm{LOS})[\mathrm{dB}](d) = 69.8 + 20\log_{10}(d) + X_\sigma(\sigma = 4.8\ \mathrm{dB}) \quad (8)$$

$$\mathrm{PL}_{73\mathrm{GHz\text{-}Hybrid}}(\mathrm{NLOS})[\mathrm{dB}](d) = 69.8 + 34\log_{10}(d) + X_\sigma(\sigma = 7.9\ \mathrm{dB}) \quad (9)$$

$$\mathrm{PL}_{73\mathrm{GHz\text{-}Access}}(\mathrm{LOS})[\mathrm{dB}](d) = 69.8 + 20\log_{10}(d) + X_\sigma(\sigma = 5.2\ \mathrm{dB}) \quad (10)$$

$$\mathrm{PL}_{73\mathrm{GHz\text{-}Access}}(\mathrm{NLOS})[\mathrm{dB}](d) = 69.8 + 33\log_{10}(d) + X_\sigma(\sigma = 7.6\ \mathrm{dB}) \quad (11)$$

$$\mathrm{PL}_{73\mathrm{GHz\text{-}Backhaul}}(\mathrm{LOS})[\mathrm{dB}](d) = 69.8 + 20\log_{10}(d) + X_\sigma(\sigma = 4.2\ \mathrm{dB}) \quad (12)$$

$$\mathrm{PL}_{73\mathrm{GHz\text{-}Backhaul}}(\mathrm{NLOS})[\mathrm{dB}](d) = 69.8 + 35\log_{10}(d) + X_\sigma(\sigma = 7.9\ \mathrm{dB}) \quad (13)$$

The corresponding floating-intercept NLOS omnidirectional path loss models for 28 GHz and 73 GHz and specified for T-R separation distances between 30 m and 200 m are shown in the following equations.

$$\mathrm{PL}_{28\mathrm{GHz}}(\mathrm{NLOS})[\mathrm{dB}](d) = 79.2 + 26\log_{10}(d) + X_\sigma(\sigma = 9.6\ \mathrm{dB}) \quad (14)$$

$$\mathrm{PL}_{\text{73GHz-Hybrid}}(\mathrm{NLOS})[\mathrm{dB}](d) = 80.6 + 29\log_{10}(d) + X_\sigma(\sigma = 7.8\ \mathrm{dB}) \quad (15)$$

$$\mathrm{PL}_{\text{73GHz-Access}}(\mathrm{NLOS})[\mathrm{dB}](d) = 81.9 + 27\log_{10}(d) + X_\sigma(\sigma = 7.5\ \mathrm{dB}) \quad (16)$$

$$\mathrm{PL}_{\text{73GHz-Backhaul}}(\mathrm{NLOS})[\mathrm{dB}](d) = 84.0 + 28\log_{10}(d) + X_\sigma(\sigma = 7.8\ \mathrm{dB}) \quad (17)$$

## VI. Conclusion

New 28 GHz and 73 GHz omnidirectional path loss models were presented which may be used in next generation mmWave radio-system design, invaluable in standards work. The omnidirectional models show that the NLOS path loss exponents for both 28 GHz and 73 GHz are the same, $\overline{n}$ = 3.4. The 28 GHz and 73 GHz measurements showed that mmWave channels are more directional at both the TX and RX than conventional UHF/Microwave channels, as a result of less prominent weaker diffuse scattering in mmWave channels. While omnidirectional path loss models are currently in use, the promise of beamforming and beam combining technologies at the mobile handset using electrically-phased on-chip antenna arrays will require mmWave directional path loss models that allow one to estimate the received power level in a narrow given direction [16]–[19].

## VII. Acknowledgement

This project was supported by the following NYU WIRELESS Industrial Affiliates: AT&T, Ericsson, Huawei, Intel, L-3 Communications, National Instruments, Nokia, Qualcomm, Samsung Group, and Straight Path Communications Inc. This project was also supported by the GAANN Fellowship program.

## References

[1] 3GPP, "Spatial channel model for multiple input multiple output (mimo) simulations," Sept 2012.

[2] 3GPP, "Spatial channel model for multiple input multiple output (mimo) simulations," 3rd Generation Partnership Project (3GPP), TR 25.996, Sep 2003. [Online]. Available: http://www.3gpp.org

[3] P. Kyosti and et al., "WINNER II channel models," European Commision, IST-WINNER, Tech. Rep. D1.1.2, Sep 2007. [Online]. Available: http://projects.celticinitiative.org/winner+/WINNER2-Deliverables/

[4] M. K. Samimi and T. S. Rappaport, "Ultra-wideband statistical channel model for non line of sight millimeter-wave urban channels," in *Global Telecommunications Conference (GLOBECOM 2014), 2014 IEEE, Accepted*, Dec 2014.

[5] T. S. Rappaport, S. Sun, R. Mayzus, H. Zhao, Y. Azar, K. Wang, G. N. Wong, J. K. Schulz, M. Samimi, and F. Gutierrez, "Millimeter Wave Mobile Communications for 5G Cellular: It Will Work!" *IEEE Access*, vol. 1, pp. 335–349, 2013.

[6] Y. Azar, G. N. Wong, K. Wang, R. Mayzus, J. K. Schulz, H. Zhao, F. Gutierrez, D. Hwang, and T. S. Rappaport, "28 GHz propagation measurements for outdoor cellular communications using steerable beam antennas in New York City," in *International Conference on Communications (ICC), 2013 IEEE*, June 2013, pp. 5143–5147.

[7] G. R. MacCartney and T. S. Rappaport, "73 GHz millimeter wave propagation measurements for outdoor urban mobile and backhaul communications in New York City," in *International Conference on Communications (ICC), 2014 IEEE*, June 2014.

[8] S. Hur, N. G. Kang, J. Park, J. A. Lee, Y. J. Cho, and M. Nekovee, "Millimeter-wave channel modeling on 28 GHz," *COST IC1004*, Feb 2014.

[9] CISCO, "Cisco visual networking index: Mobile data traffic forecast update, 2013-2018," 2014.

[10] M. Samimi, K. Wang, Y. Azar, G. N. Wong, R. Mayzus, H. Zhao, J. K. Schulz, S. Sun, F. Gutierrez, and T. S. Rappaport, "28 GHz angle of arrival and angle of departure analysis for outdoor cellular communications using steerable beam antennas in New York City," in *Vehicular Technology Conference (VTC Spring), 2013 IEEE 77th*, June 2013, pp. 1–6.

[11] T. S. Rappaport, *Wireless Communications: Principles and Practice*, 2nd ed. Upper Saddle River, NJ: Prentice Hall, 2002.

[12] G. R. MacCartney, J. Zhang, S. Nie, and T. S. Rappaport, "Path loss models for 5G millimeter wave propagation channels in urban microcells," in *Global Telecommunications Conference (GLOBECOM 2013), 2013 IEEE*, Dec 2013.

[13] P. Kysoti, J. Meinila, L. Hentila, and *et al.*, "WINNER II Channel Models," CEC, Tech. Rep. IST-4-027756, 2008.

[14] S. Rangan, T. S. Rappaport, and E. Erkip, "Millimeter-wave cellular wireless networks: Potentials and challenges," *Proceedings of the IEEE*, vol. 102, no. 3, pp. 366–385, March 2014.

[15] M. Feuerstein, K. Blackard, T. Rappaport, S. Seidel, and H. Xia, "Path loss, delay spread, and outage models as functions of antenna height for microcellular system design," vol. 43, no. 3, Aug 1994, pp. 487–498.

[16] F. Gutierrez, T. S. Rappaport, and J. Murdock, "Millimeter-wave CMOS antennas and RFIC parameter extraction for vehicular applications," in *Vehicular Technology Conference Fall (VTC 2010-Fall), 2010 IEEE 72nd*, Sept 2010, pp. 1–6.

[17] S. Sun and T. S. Rappaport, "Multi-beam antenna combining for 28 GHz cellular link improvement in urban environments," in *Global Communications Conference (GLOBECOM), 2013 IEEE*, Dec 2013.

[18] S. Sun, G. R. MacCartney, M. Samimi, S. Nie, and T. S. Rappaport, "Millimeter wave multi-beam antenna combing for 5G cellular link improvement," in *International Conference on Communications (ICC), 2014 IEEE*, June 2014.

[19] S. Sun and T. S. Rappaport, "Wideband mmwave channels: Implications for design and implementation of adaptive beam antennas," in *International Microwave Symposium (IMS), 2014 IEEE*, June 2014.